Fluid vortex mapping using the rotational Doppler effect

O. Emile, Janine Emile

HAL Id: hal-03687802
https://hal.science/hal-03687802

Fluid vortex mapping using the rotational Doppler effect.

Olivier EMILE

Université de Rennes 1, Campus de Beaulieu, F-35000 Rennes, France

Janine EMILE

Université de Rennes 1, CNRS IPR UMR 6251, F-35000 Rennes, France

Abstract

The light from a twisted laser beam, scattered at an air/water interface, experiences a rotational Doppler shift. We use a superposition of two beams with different topological charges to measure the beat frequency of the scattered light at different distances from the vortex centre. We show that the angular velocity decreases with the distance and we identify this vortex as being from the Rankine type. Several extensions are then considered including the detection of turbulences generated in the wake of aeroplanes.

Keywords: Light orbital angular momentum, Rotational Doppler effect, Rankine vortex.

2020 MSC: 78A45, 78A60, 78A10.

1. Introduction

Vortices are ubiquitous in everyday life. We all came across them, whether by tolling our coffee, or contemplating the siphon of a sink or even gazing at atmospheric turbulences such as those generated by planes or cyclones. They can also been encountered in physics in very large systems such as in the accretion

---

*Corresponding author

Email addresses:* `emile@univ-rennes1.fr` (Olivier EMILE),
`janine.emile@univ-rennes1.fr` (Janine EMILE)

of black holes [1] or in purely quantum phenomena such as in superfluid helium in a rotating container [2] or irotating Bose Einstein condensates [3]. And yet, as pointed out by R. Feynman about turbulences [4]: it is *the most important unsolved problem of classical physics*. From an experimental point of view, vorticity is usually estimated from a number of velocity field measurements at several points near the point of interest, which then allow computation of the velocity derivatives over space. This could be achieved through Laser Doppler Velocimetry, Particle Image Velocimetry, or Molecular Tagging Velocimetry, for example [5, 6]. These methods then provide an indirect measurement of vorticity by reconstruction of the velocity field. On the other hand, vortices can be found in electromagnetic waves [7, 8] especially via the Orbital Angular Momentum (OAM). One may then wonder whether fluid vortices could be probed using OAM.

In particular, waves carrying OAM can experience a so-called rotational Doppler shift [9], as the source and the receiver are rotating regarded to each other. Moreover, in order to observe rotational Doppler shifts, the topological charge of the OAM beam has to change during interaction [10]. It has been used to detect light reflected from dedicated rotating objects such as phase conjugate mirrors [11], prisms [12] or metasurfaces [13], or on the decomposition of the light behind a rotating object [14, 15]. Besides, the OAM scattered light by a rough object [16, 17] or by scatters in a rotating fluid at the focus of a laser [18] also experiences a rotational Doppler shift. One may then wonder whether it could be possible to characterize the whole vortex using OAM. The aim of this letter is to investigate a fluid vortex and to map its rotational structure using the rotational Doppler shift, taking advantages of the diffusion by the fluid itself.

2. Experimental set-up

To that purpose we have built the following experimental set-up. The green laser light from a He-Ne laser (Melles Griot $\lambda = 543$ nm, P=2 mW) is trans-

2

formed to a superposition of two Laguerre Gaussian modes with topological charges $\ell_1 = 1$ and $\ell_2 = 2$, thanks to a Spiral Phase Plate (SPP) ($\lambda = 633$ nm, RC photonics). Actually, the use of such a SPP generates a beam with a fractional topological charge ($\ell = 1.15$) [19], which can be decomposed in two major modes, a predominant $\ell_1 = 1$ mode and a $\ell_2 = 2$ mode [20, 21]. Such a beam has a rather cylindrical symmetry with no intensity in its center, the light being concentrated on a ring. The beam is then expanded using two lenses, f_1 and f_2 (see Fig. 1). The lens f_2 can be moved to adjust the beam size (radius of maximum light intensity) on the air/liquid interface. In all the experiments the liquid is here water.

The liquid rotation is not necessarily uniform. It varies with the distance r to the rotation axis. Let us call $\nu_{rot}(r)$ its rotation frequency. We generate this movement either by rotating a tank and thus the whole liquid at a constant velocity (referenced hereafter as exp. 1), or by using a magnetic stirrer that generates a vortex in the liquid (exp. 2, see Fig. 1). In this later case, special care is taken to align the centre of the liquid vortex with that of the laser beam. We then collect the light scattered at the air/liquid interface. Due to the interaction process, the scattered light doesn't carry OAM any more [16, 17, 18]. Thus, the scattered light experiences a rotational Doppler frequency shift $\triangle\nu$ [9]

$$\triangle\nu = \ell\nu_{rot}(r) \tag{1}$$

We then look here for a beat frequency between the two modes at a frequency that should equal $(\ell_2 - \ell_1)\nu_{rot}(r) = \nu_{rot}(r)$.

We could have used a superposition of ℓ and $-\ell$ modes, with high values of ℓ as it is usually performed [16, 17, 18]. However, we choose to use low order modes since they can be easily handled. In particular the divergence of the beam is lower [22]. Besides a low order superposition of ℓ and $-\ell$ ($\ell = 1$ or $\ell = 2$) has a cartesian symmetry and is more difficult to align. We could also have used a single Laguerre gaussian beam as it is managed in numerical experiments simulating vortices [23]. This would imply the use of acousto-optic modulators
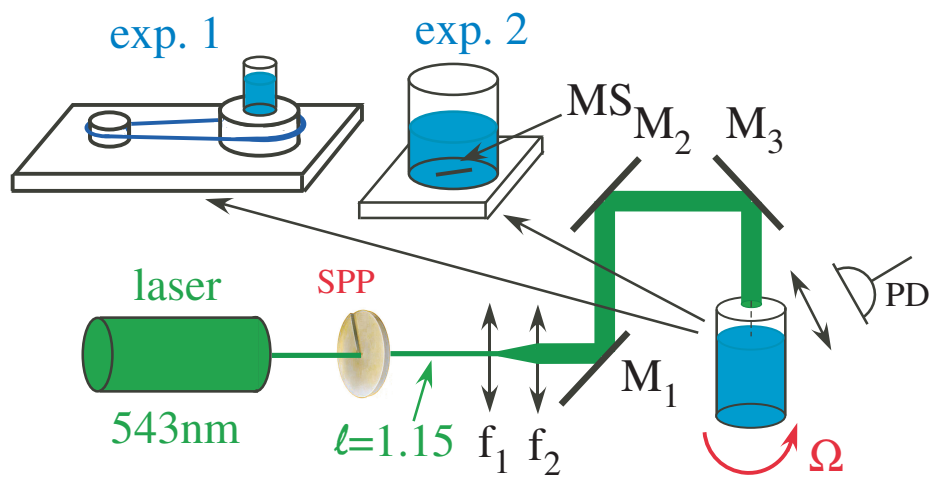
3

Figure 1: Experimental set-up. The fundamental mode of a He-Ne green laser ($= 543$ nm) is transformed to a superposition of a $\ell_1 = 1$ and $\ell_2 = 2$ Laguerre Gaussian beam with a $\lambda = 633$ nm-SPP (see text). The light is diffracted at a rotating air/water interface and collected on a photodiode (PD), investigating the beat frequency between the shifted modes. f_1 and f_2 lenses focal with lengths 5 and 30 cm respectively. The liquid is set in rotation either by the rotation of a tank (exp. 1) or via a magnetic stirrer MS (exp. 2).

to perform an heterodyne measurement. Finally, the use of a $\ell = 1.15$ beam, combination of $\ell_1 = 1$ and $\ell_2 = 2$ as explained above, seems to be here a good compromise. It keeps a good cylindrical symmetry and is easy to handle.

3. Results

In order to validate the experimental procedure we first perform the experiment on a uniform rotation of a liquid in a rotating tank (exp. 1 in Fig. 1). The tank is inserted in a home made shaft set in rotation at a frequency ν_t by a belt and a motor. The centre of the beam is carefully aligned with the axis of the rotation. For a given rotation frequency of the tank, we measure the frequency modulation that corresponds to the beat frequency ν_b between the two main modes. We check, by changing the size of the probing beam that the fluid rotation is uniform. We then vary the rotation frequency and record the beat frequency (see Fig. 2). This variation is linear with a slope equal to one. There is a perfect correspondence between the rotation frequency of the fluid $\nu_{rot}(r)$, the rotation frequency of the tank $\nu - t$ and the beat frequency ν_b observed on the photodiode.

We then apply this Doppler rotational shift technics to a vortex in a liquid (exp. 2 in Fig. 2). We use a magnetic stirrer in a 50 ml tank (inner diameter 40 mm) to generate a vortex. The stirrer is 20 mm long. We adjust the rotating frequency of the stirrer in order to obtain a steady state vortex with a uniform rotation of the stirrer. The rotation frequency of the stirrer ν_0 is measured independently with a camera. As previously, we measure the modulation of the scattered signal from the surface that corresponds to the beat frequency between the two modes. As already mentioned, the probed zone is a circle of radius r that corresponds to the maximum intensity of the laser light. The beat frequency equals the angular rotation $\nu_{rot}(r)$ at radius r. This zone can be modified by changing the distances between the two lenses. We measure the circle radius r and we register the corresponding signal modulation. The results appear in Fig. 3.
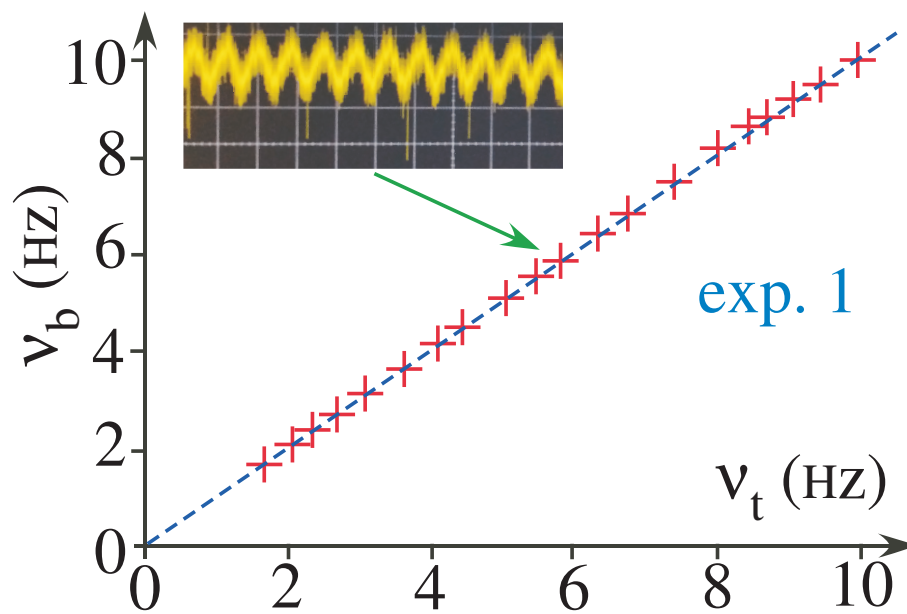
5

Figure 2: Variation of the beat frequency between the $\ell = 1$ and $\ell = 2$ modes versus the rotation of the tank. The size of the crosses corresponds to the error bars. The dotted line is a linear adjustment. Inset: recorded beat frequency for a rotation of the stirrer $\nu_t = 5.95$ Hz. Scale: 200 ms/div.
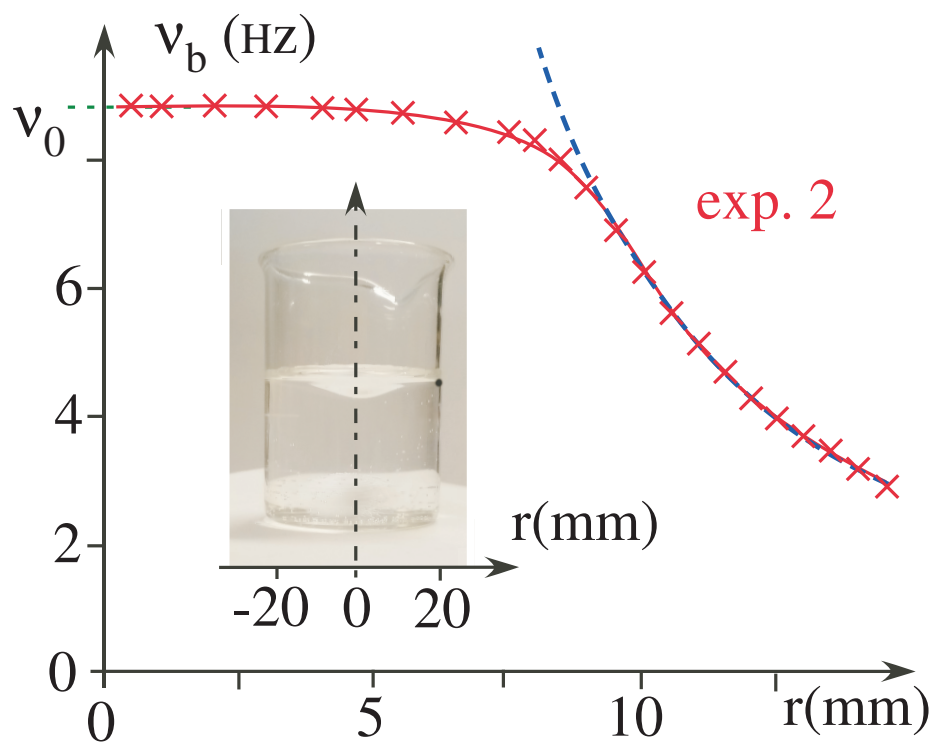
Figure 3: Measured scattered light modulation frequency ν_b corresponding to the beat frequency versus the radius of maximum intensity of the laser light, for a given rotation frequency of the stirrer ν_0. The error bars corresponds to the size of the crosses. The solid line is a guide for the eye. Dotted line: theoretical adjustment according to Eq. 2. Insert: picture of the vortex showing the shape of the water surface due to the vortex.

4. Discussion

4.1. Vortex circulation strength

Obviously, the technics we developed here makes it possible to carry out a complete mapping of the rotation of the surface of the vortex. Close to the centre of it, the angular velocity is constant. It equals the rotation frequency of the stirrer ν_0. It then decreases as we leave the central region. This kind of vortex resembles the so-called Rankine vortex [24, 25]. Actually, the liquid flow generated by a magnetic stirrer in a container is well approximated by a Rankine vortex [26]. In such a vortex, the circulation strength Γ equals

$$\Gamma_0 = 2\pi\omega_{rot}(r)r^2 \tag{2}$$

where $\omega_{rot}(r) = 2\pi\nu_{rot}(r)$ is the angular rotation at a distance r from the vortex centre. This expression holds out of a radius a ($r \geq a$), a being a constant distance characteristic of the vortex. Experimentally we have measured $a \simeq 8$ mm. When $r \leq a$, the angular velocity is constant. It corresponds to the rotation frequency of the stirrer ν_0. For the $r \geq a$ region, we have performed a theoretical adjustment of the experimental data of Fig. 3, according to Eq. 2 (see dotted line). The agreement is very good. The vortex is definitely a Rankine type vortex [24, 25]. We find a circulation strength that equals $\Gamma_0 = (12.3 \pm 0.3) \times 10^{-3}$ m^2/s. The finite size of the tank has little influence on the vortex behavior.

We have also plotted the variation of the vortex circulation strength Γ_0 versus the rotation frequency of the stirrer, in a range where we could reach a steady state rotation of the vortex (see Fig. 4). Within this small angular velocity range, the vortex strength seems to vary linearly with the central angular velocity, which is imposed by the rotation of the magnetic stirrer. The slope of this straight line is equal to $(1.55 \pm 0.04) \times 10^{-3}$ m^2. The value of a seems to be constant within this small range.

8
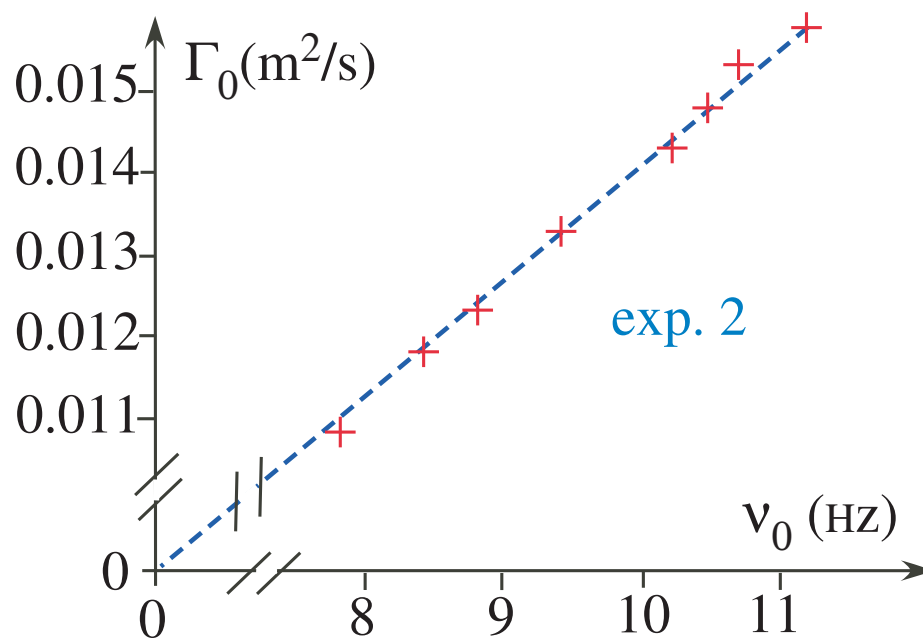
Figure 4: Variation of the vortex circulation strength Γ_0 versus the rotation frequency of the stirrer (ν_0). The dotted line is a linear adjustment of the experimental points.

4.2. Applications

The investigation of the vortex has been here performed using a combination of $\ell_1 = 1, \ell_2 = 2$, in order to easily handle and focus the beam at the air/water interface. Then the beat frequency of the scattered light ν_b equals to the rotation frequency ν_r $(\nu_b = (\ell_2 - \ell_1)\nu_r)$. The probing of the different distance has been achieved step by step, by changing the distance between the lenses, in order to clearly demonstrate the experimental procedure. However, for practical applications, the whole measurements need to be performed at the same time or on a small time scale compared to the characteristic evolution time of the vortex.

For example, the measurement could have been done by using several non overlapping superpositions of ℓ and $-\ell$ beam, with different wavelengths. The wavelength demultiplexing would give access to the rotational Doppler shift for a given radius for each wavelength at the same time. Moreover, if one uses a superposition of ℓ and $-\ell$, the beat frequency then equals $\nu_b = 2\ell\nu_r$ [16, 17, 18]. For a $\ell = 50$ for example, ν_b would be in the kHz range. Then, the measurement of the shift could be performed on a smaller time. From the signal processing point of view, it would be much easier to deal with. Besides with a higher topological charge value, the light intensity would be concentrated on a smaller ring that would more precisely define the radius of the vortex to be probed.

Most of the technics developed to identify vortices up to now, use test particles to indirectly reveal the vortex pattern. However, the presence of particles within the vortex may change its characteristics and behavior. For example, we have tried to add metallic micro-particles to enhance the scattered light signal. Due to the centrifugal forces, the particles aggregate and rotate at a much smaller frequency as the liquid. The use of a superposition of Laguerre Gaussian beam could be an alternative and a versatile technics to directly identify vortices.

One may yet wonder whether the rotational Doppler measurement could alter the vortex. Actually, as pointed out in [9], the rotational Doppler effect is associated with exchange of energy between light and matter, due to energy

10

conservation. Nevertheless, the torque exerted by the light on the fluid equals $N\hbar$, where $N = P/(h\nu)$ is the number of photon per second, P being the optical power, and $h = 2\pi\hbar$ the Plank constant. For a 1 mW laser light, the torque is thus of the order of 10^{-19} kgm^2/s, whereas for a 20 ml of water, the torque generated by the stirrer is of the order of 2×10^{-4} kgm^2/s. Besides, for opposite values of ℓ, the energy variation of the rotating body du to the Doppler effect cancels [27]. One has also to note that for green light the absorption of radiation by water here is negligible.

5. Conclusion

We have developed a technics that use the rotational Doppler effect to investigate the structure of a vortex. We use a superposition of Laguerre Gaussian modes with different topological charges as incident light. We collect the scattered light from the air/water interface. The modulation of the intensity signal corresponds to the beat frequency between the frequency shifted modes. It is thus proportional to the rotation frequency of the liquid. As a proof of concept, we have first probed the uniform rotation of water in a rotating tank. We have then performed a surface mapping of the vortex generated by a magnetic stirrer in a tank. We have clearly identified a so-called Rankine like vortex.

This technics is not restricted to liquid vortices. It can be applied to any vortex including dust devil [28], tornados [29], or in the wake generated by planes either in take off, or landing or during flight [30]. The particle image velocimetry or the transverse Doppler velocity detection by lidar radar [31] for example would be then be supplemented by the scattered light detection in the axis of the vortex, giving directly access to the rotational structure of the vortex. Coupled with a time of flight technics using a pulsed laser, one would be able to investigate the structure of the wake at different distances, performing a three dimensional investigation.

11

Acknowledgements

References

[1] A. Ingram, M. van der Klis, M. Middleton, C. Done, D. Altamirano, L. Heil, P. Uttley, M. Axelsson, A quasi-periodic modulation of the iron line centroid energy in the black hole binary H1743- 322, Mon. Not. R. Astron. So. 461 (2) (2016) 1967–1980.

[2] G. P. Bewley, D. P. Lathrop, K. R. Sreenivasan, Visualization of quantized vortices, Nature 441 (7093) (2006) 588–588.

[3] M. R. Matthews, B. P. Anderson, P. Haljan, D. Hall, C. Wieman, E. A. Cornell, Vortices in a bose-einstein condensate, Phys. Rev. Lett. 83 (13) (1999) 2498.

[4] R. P. Feynman, R. B. Leighton, M. L. Sands, The Feynman Lectures on Physics, Pearson/Addison-Wesley, Boston, USA, 2006.

[5] C. Tropea, A. L. Yarin, J. F. Foss, eds, Handbook of experimental fluid mechanics, Vol. 1, Springer Berlin, 2007.

[6] J.-H. Feng, C.-B. Shen, Q.-C. Wang, Three-dimensional evolution of large-scale vortices in supersonic flow, Appl. Phys. Lett. 107 (2015) 254101.

[7] G. Molina-Terriza, J. P. Torres, L. Torner, Twisted photons, Nat. Physics 3 (5) (2007) 305–310.

[8] B. Thidé, F. Tamburini, OAM Radio–physical foundations and applications of electromagnetic orbital angular momentum in radio science and technology, John Wiley and Sons, 2021.

[9] L. Fang, M. J. Padgett, J. Wang, Sharing a common origin between the rotational and linear doppler effects, Laser Photon. Rev. 11 (6) (2017) 1700183.

[10] M. Mansuripur, Angular momentum exchange between light and material media deduced from the doppler shift, in: Optical Trapping and Optical Micromanipulation IX, Vol. 8458, 2012, p. 845805.

[11] A. Y. Okulov, Rotational doppler shift of a phase-conjugated photon, J. Opt. Soc. Am. B 29 (4) (2012) 714–718.

[12] O. Emile, J. Emile, C. Brousseau, Rotational doppler shift upon reflection from a right angle prism, Appl. Phys. Lett. 116 (22) (2020) 221102.

[13] P. Georgi, C. Schlickriede, G. Li, S. Zhang, T. Zentgraf, Rotational doppler shift induced by spin-orbit coupling of light at spinning metasurfaces, Optica 4 (8) (2017) 1000–1005.

[14] W. Zhang, J. Gao, D. Zhang, Y. He, T. Xu, R. Fickler, L. Chen, Free-space remote sensing of rotation at the photon-counting level, Phys. Rev. Applied 10 (2018) 044014.

[15] O. Emile, J. Emile, C. Brousseau, T. le Guennic, P. Jian, G. Labroille, Rotational doppler shift from a rotating rod, Opt. Lett. 46 (15) (2021) 3765–3768.

[16] M. P. Lavery, F. C. Speirits, S. M. Barnett, M. J. Padgett, Detection of a spinning object using lights orbital angular momentum, Science 341 (6145) (2013) 537–540.

[17] M. P. Lavery, S. M. Barnett, F. C. Speirits, M. J. Padgett, Observation of the rotational doppler shift of a white-light, orbital-angular-momentum-carrying beam backscattered from a rotating body, Optica 1 (1) (2014) 1–4.

[18] A. Ryabtsev, S. Pouya, A. Safaripour, M. Koochesfahani, M. Dantus, Fluid flow vorticity measurement using laser beams with orbital angular momentum, Opt. Express 24 (11) (2016) 11762–11767.

13

[19] O. Emile, C. Brousseau, J. Emile, R. Niemiec, K. Madhjoubi, B. Thide, Electromagnetically induced torque on a large ring in the microwave range, Phys. Rev. Lett. 112 (5) (2014) 053902.

[20] M. V. Berry, Optical vortices evolving from helicoidal integer and fractional phase steps, J. Opt. A: Pure Appl. Opt. 6 (2) (2004) 259–268.

[21] J. B. Götte, K. O'Holleran, D. Preece, F. Flossmann, S. Franke-Arnold, S. M. Barnett, M. J. Padgett, Light beams with fractional orbital angular momentum and their vortex structure, Opt. Express 16 (2) (2008) 993–1006.

[22] M. J. Padgett, F. M. Miatto, M. P. J. Lavery, A. Zeilinger, R. W. Boyd, Divergence of an orbital-angular-momentum-carrying beam upon propagation, New J. Phys. 17 (2) (2015) 023011.

[23] A. Belmonte, C. Rosales-Guzmán, J. P. Torres, Measurement of flow vorticity with helical beams of light, Optica 2 (11) (2015) 1002–1005.

[24] D. Acheson, F. D. Acheson, Elementary Fluid Dynamics, Oxford University Press, 1990.

[25] N. D. Katopodes, Chapter 7 - Vorticity Dynamics, in: N. D. Katopodes (Ed.), Free-Surface Flow, Butterworth-Heinemann, 2019, pp. 516–565.

[26] G. Halász, B. Gyüre, I. M. Jánosi, K. G. Szabó, T. Tél, Vortex flow generated by a magnetic stirrer, Am. J. Phys. 75 (12) (2007) 1092–1098.

[27] O. Emile, J. Emile, Energy, linear momentum, and angular momentum of light: What do we measure?, Ann. Phys. 530 (12) (2018) 1800111.

[28] R. D. Lorenz, M. R. Balme, Z. Gu, H. Kahanpää, M. Klose, M. V. Kurgansky, M. R. Patel, et al., History and applications of dust devil studies, Space Sci. Rev. 203 (1) (2016) 5–37.

[29] L. Wu, Q. Liu, Y. Li, Prevalence of tornado-scale vortices in the tropical cyclone eyewall, Proc. Natl. Acad Sci. USA 115 (33) (2018) 8307–8310.

14

[30] T. Gerz, F. Holzpfel, D. Darracq, Commercial aircraft wake vortices, Progr. Aerosp. Sci. 38 (3) (2002) 181–208.

[31] A. Dolfi-Bouteyre, G. Canat, M. Valla, B. Augere, C. Besson, D. Goular, L. Lombard, J.-P. Cariou, A. Durecu, D. Fleury, et al., Pulsed 1.5-μm lidar for axial aircraft wake vortex detection based on high-brightness large-core fiber amplifier, IEEE J. Sel. Top. Quantum Electron. 15 (2) (2009) 441–450.

260